Tailoring of optical mode profiles of high-power diode lasers evidenced by near-field photocurrent spectroscopy

Anna Kozlowska,[a)] Michał Szymański, Emilia Pruszyńska-Karbownik, and Maciej Bugajski
Institute of Electron Technology, Al. Lotników 32/46, 02-668 Warsaw, Poland

Robert Pomraenke and Christoph Lienau
Institut für Physik, Carl von Ossietzky Universität, 26111 Oldenburg, Germany and Max-Born Institut, Max-Born-Str. 2 A, 12489 Berlin, Germany

Julien Renard
Equipe CEA-CNRS-UJF Nanophysique et Semiconducteurs, DRFMC/SP2M/PSC, CEA-Grenoble, 17 rue des Martyrs, 38054 Grenoble Cedex 9, France and Max-Born Institut, Max-Born-Str. 2 A, 12489 Berlin, Germany

Andrzej Maląg
Laser Laboratory, Institute of Electronic Materials Technology, 133 Wolczynska St., 01-919 Warsaw, Poland

Tailoring of optical mode profiles of high-power diode lasers is directly demonstrated by means of near-field photocurrent spectroscopy. Three double barrier separate confinement heterostructures with different confinement geometries are designed and their optical mode profiles are studied both theoretically and experimentally. The near-field spectroscopic results clearly resolve the intended variation in optical mode width. A remaining discrepancy between the designed and experimentally measured mode profiles, manifesting itself in the reduction of their evanescent tails, is attributed to the structure of the antiguiding barrier. The results demonstrate that near-field field photocurrent spectroscopy is a powerful, nondestructive, and quantitative technique for optical waveguide inspection in high-power diode lasers. © *2007 American Institute of Physics.*
[DOI: 10.1063/1.2779846]

The tailoring of optical mode profiles of diode lasers plays an important role in device optimization, providing a possibility to improve the laser beam quality and to influence the optical power distribution at the facets. Optimized facet distributions are particularly important for high-power devices, where high energy densities at the facets limit the achievable optical power due to catastrophic optical damage. Modifications of the waveguide design can result in a significant increase of the device output power,[1,2] and detailed knowledge about the optical field distributions is therefore of paramount importance. Because of the small, submicron dimensions of these waveguide structures, optical mode profiles are difficult to measure directly and usually they are determined indirectly from far-field directional distributions. More detailed information can be obtained by near-field optical spectroscopy (NSOM),[3,4] which overcomes the diffraction limit of optical imaging and thus allows for a highly spatially resolved characterization of optoelectronic devices. Consequently, this method has been used for various analyses of the spatial emission properties of diode lasers.[5,6] Specifically, a direct imaging of optical mode profiles of semiconductor diode lasers was demonstrated[7] by using near-field photocurrent (NPC) spectroscopy.[8,9]

In this letter, we use near-field photocurrent spectroscopy for directly demonstrating the tailoring of optical mode profiles of high-power diode lasers. Three double barrier separate confinement heterostructures (DB SCH) with different confinement geometries were designed and their optical mode profiles were studied both theoretically and experimen-

tally. The experimental results do not only verify the predicted design trends but provide, moreover, a precise, quantitative measurement of the mode profiles, thereby giving valuable information about the waveguide properties in operating optoelectronic devices.

The conceptual idea for tailoring mode profiles is illustrated in Fig. 1(a). In GaAs-based DB SCH heterostructures, aluminum barriers at the interface between waveguide and cladding layers enable one to separately control both carrier and optical confinement.[10] We have designed three versions of such structures, labeled A, B, and C, differing in barrier and waveguide composition and thickness. A modeling of the optical mode profiles of the as-designed structures was per-
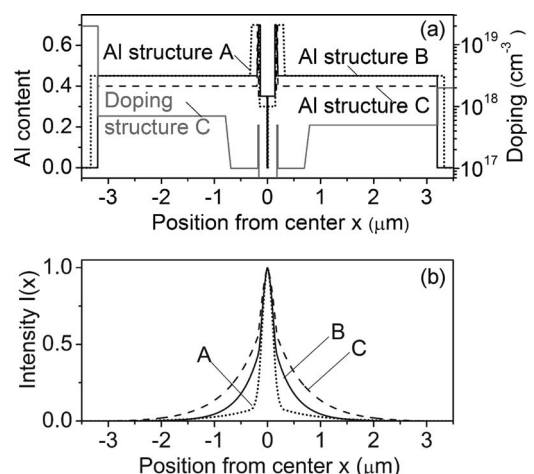

FIG. 1. (a) Design values for the spatial distribution of the Al content and doping level of three different types (A–C) of DB SCH heterostructures. (b) Theoretically predicted optical mode profiles for these three designs.

[a)]Author to whom correspondence should be addressed; electronic mail: kozlowsk@ite.waw.pl

formed using the Photon Design software.[11] This modeling shows that a local antiguiding is introduced at the barrier-cladding interface, leading to a weakening of optical confinement. This results in non-Gaussian optical mode profiles $I(x)$ with a different degree of penetration of the evanescent tails of $I(x)$ into the cladding layer [Fig. 1(b)]. These tails are fairly weak for version A, but can largely be enhanced by varying the diode design. From these mode profiles, we calculated beam divergences of 11.6°, 14.2°, and 11.2° full width at half maximum (FWHM) for designs A–C, respectively. Such low beam divergences are of considerable interest for many applications of diode lasers, making a detailed experimental analysis of their optical waveguide properties highly relevant.

Based on these three designs, different heterostructures have been grown on an n-type GaAs substrate by low pressure metal-organic vapor-phase epitaxy. The tensile-strained 15 nm thick GaAsP quantum well (QW) used as the active layer was optimized for emission at $\lambda_0 = 808$ nm. Wide-stripe ($w = 0.1$ mm), gain guided laser structures were fabricated by He$^+$ implantation for stripe definition. TiPt and AuGeNi metallizations were used as p and n contacts, respectively. Lasers of cavity length $L = 1$ mm were formed by cleaving and subsequent low and high reflection facet coating (AlN–Si/AlN, refractive index $n_{AR} = 1.9$). Three representative diode lasers, labeled a, b, and c from designs A, B, and C, respectively, were investigated in this work.

Near-field photocurrent images were recorded using a previously described NSOM system.[12] As near-field probe, we used an aluminium-coated fiber tip with an aperture of the order of 100 nm which was scanned at a constant distance of ~10 nm across the laser diode facet, using a shear force feedback setup. A He–Ne or a tunable Ti:Sapphire laser, chopped at a frequency of 2.75 kHz, was coupled into the near-field fiber and used as a local excitation source. The photocurrent signal from the unbiased diode laser was recorded as a function of tip position using lock-in detection.

The investigated laser diodes were characterized using various far-field techniques. The measured far-field optical beam divergences were 22°, 17°, and 13° for the devices a–c, respectively, substantially larger than the predicted values. Macroscopic photocurrent (PC) spectroscopy showed a steep PC onset at 1.53 eV due to interband absorption from 11 h to 1e levels within the QW.[13] A further absorption edge at 1.85 eV arises from interband transitions within the laser waveguide. Defect-related transitions manifest themselves in a faint shoulder at energies below 1.53 eV.

Figure 2 shows one-dimensional NPC scans $I_{NPC}(x)$ for diodes a–c, recorded by scanning the tip along the x axis, perpendicularly to the junction, at various excitation wavelengths between 633 and 820 nm. All curves show maxima in the active region of the heterostructure ($x = 0$). The interface between heterostructure and substrate can be discerned in Fig. 2(a) at $x \approx 3$ μm.

In the following, we will interpret the NPC scans shown in Fig. 2. For this purpose, we have to consider the local interaction between the optical field of the probe and the different absorbing regions of the heterostructure. For wavelengths close to λ_0, laser wavelength comes from carriers generated by interband absorption inside the QW.[7,9] In this wavelength region, both defect-related absorption and absorption by the AlGaAs waveguide layers are too weak to contribute significantly.[7,9] Here, the NPC scans represent the
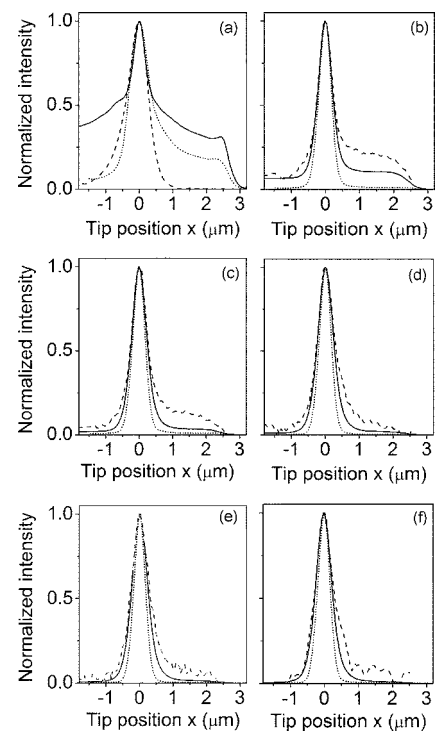

FIG. 2. NPC line scans in the direction perpendicular to the junction for the diode lasers a (dotted line), b (solid line), and c (dashed line) recorded for different excitation wavelengths: (a) 633 nm, (b) 775 nm, (c) 800 nm, (d) 810 nm, (e) 815 nm, and (f) 820 nm.

profile of the fundamental waveguide mode.[7] For excitation at $\lambda = 633$ nm, however, also the Al$_{0.3}$Ga$_{0.7}$As (device a) and Al$_{0.35}$Ga$_{0.65}$As (devices b and c) waveguide regions contribute to the NPC signal, in addition to the QW contribution. The modeling also shows for all diodes that at this wavelength higher order waveguide modes can be excited, giving an additional contribution to the photocurrent. When increasing the excitation wavelength toward λ_0, these additional contributions decrease continuously [Figs. 2(b)–2(d)], so that at around 810 nm the near-field image essentially exclusively reflects the fundamental mode. With further increase in excitation wavelength, the optical field coupled into the waveguide penetrates deeper into the laser structure. In these cases, defect transitions outside the waveguide may contribute and give rise to a slight broadening of the NPC profile.[9,14] In many of the NPC profiles in Fig. 2, in particular, those at $\lambda \leq 800$ nm, a clear asymmetry can be seen. This mostly likely arises from a doping asymmetry, giving rise to variations in refractive index and thus different penetration depths of the evanescent tails of the mode profiles. This also induces a spatially asymmetric free carrier absorption, which can be another contribution to the NPC signal.

In essence, these results show that tuning the excitation wavelength λ toward 810 nm allows for the most direct imaging of the mode profiles in DB SCH heterostructures. In order to compare the experimental and theoretical results, some specific features of the NPC image contrast have to be taken into account. It has been shown previously[7] that, due to the presence of the antireflection (AR) coating protecting the laser facets, the optical field coupled via the near-field probe into the diode waveguide is mainly composed of waves propagating through the AR coating and deep into the laser diode waveguide. Evanescent waves in the AR layer decay too rapidly to contribute significantly. This essentially puts
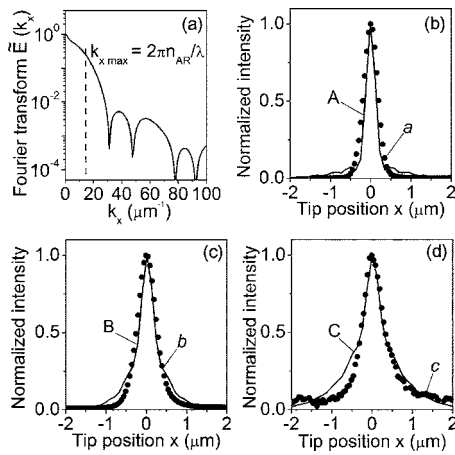
FIG. 3. (a) Fourier transform $\widetilde{E}_t(k_x)$ of the theoretical mode profile $E(x)$ of design A and maximum spatial frequency $k_{x,max}=2\pi n_{AR}/\lambda$ probed in the NPC experiments. [(b)–(d)] Simulated profiles $I_{NPC}(x)=|E_t(x)|^2$ (solid lines), calculated from truncated Fourier transforms of the theoretical mode profiles for designs A–C compared to the experimental NPC mode profiles $I_{NPC}(x)$ (circles) of the devices a–c, respectively. All NPC scans were recorded at an excitation wavelength of 810 nm.

TABLE I. FWHM beam divergences calculated (i) for the as-designed theoretical near-field distributions and (ii) from the experimental NPC traces compared to experimentally measured beam divergences (FWHM) for a series of diode lasers from the DB SCH heterostructures A–C.

Structure label	FF FWHM (deg)		Experimental FF
	Theoretical NF	NPC data	
A	11.6	21.0	22
B	14.2	16.8	17–18
C	11.2	11.2	13–14

an upper limit to the maximum transverse, i.e, parallel to the facet in x direction, component of the wave vector $k_{x,max}=2\pi n_{AR}/\lambda$ of the electric field coupled into the diode waveguide. Therefore, high frequency $k_x>k_{x,max}$ components of the electric field $E(x)$ are not resolved by our imaging technique. This is illustrated in Fig. 3(a), showing the Fourier transform $\widetilde{E}(k_x)$ of the mode profile $E(x)$ calculated for design A. Thus, a realistic strategy for quantitatively modeling the NPC profiles $I_{NPC}(x)$ consists in (i) simulating $E(x)$, (ii) calculating $\widetilde{E}(k_x)$, (iii) truncating at $k_{x,max}$, $\widetilde{E}_t(k_x)$, and (iv) back transformation to get $I_{NPC}(x)=|E_t(x)|^2$.

In Figs. 3(b)–3(d) such calculated NPC signals are compared to the experimental data. At first sight, the agreement is quite satisfactory; in particular, the predicted trend for the variation of the FWHM of the spatial mode profiles is quantitatively reproduced. Looking more closely, however, significant differences between experiment and model exist. For all three diodes, the contributions from the evanescent tails in the NPC experiments are clearly less than predicted. One certainly may take this as an indication of a yet incomplete theoretical understanding of the imaging process. Yet, there is additional independent evidence that this is not the cause of this discrepancy and that this suppression of the evanescent tails is, in fact, correctly probed by NPC. This evidence comes from calculating the far-field beam divergences from the NPC data. For multilayer semiconductor laser structures the far-field intensity at angle θ can be written in the form

$$I(\theta) = g(\theta)\left|\int_{-\infty}^{\infty} E_{NF}(x)\exp(-ik_0\sin(\theta))dx\right|^2, \quad (1)$$

where $E_{NF}(x)=\sqrt{I_{NPC}}$ is the amplitude of the near-field distribution, $k_0=2\pi/\lambda_0$, and $g(\theta)=\cos(\theta)/(n_{eff}+\cos(\theta))$ is a correction factor, accounting for the angle-dependent coupling out of the high-index semiconductor material.[15] The so-calculated beam divergences (Table I) are in remarkable agreement with the experimental far-field profilometric results. This suggests that the NPC measurements provide, in fact, a rather precise reconstruction of the near-field mode profiles and that the composition and/or thickness of the Al-

GaAs barrier layers, which largely defines the evanescent tails of the mode profiles, differs slightly from the designed values. Such variations are difficult to detect with other tools, such as photoluminescence or scanning electron microscopy, which have been used to characterize our samples. Our results thus indicate that only for structure C, for which the beam divergences based on both theoretical and experimental mode profiles are essentially identical, the barrier fully matches the design.

In summary, we have used near-field photocurrent spectroscopy to directly image the mode profiles of double-barrier separate confinement laser structures. The results show that the proposed technique is highly suited for visualizing even subtle changes in the mode profiles. In particular, the theoretically predicted variation in mode width was resolved in the experiments. A remaining discrepancy between the designed and experimental mode profiles, i.e., the reduction of their evanescent tails, is attributed to the structure of the antiguiding barrier. Our results demonstrate that near-field field photocurrent spectroscopy is a powerful, nondestructive, and quantitative technique for optical waveguide inspection in optoelectronic devices, specifically high power diode lasers.

[1] A. Knauer, G. Erbert, R. Staske, B. Sumpf, H. Wenzel, and M. Weyers, Semicond. Sci. Technol. **20**, 621 (2005).
[2] A. Maląg, A. Jasik, M. Teodorczyk, A. Jagoda, and A. Kozlowska, IEEE Photonics Technol. Lett. **18**, 1582 (2006).
[3] D. W. Pohl, W. Denk, and M. Lanz, Appl. Phys. Lett. **44**, 651 (1984).
[4] E. Betzig, J. K. Trautman, T. D. Harris, J. S. Weiner, and R. L. Kostelak, Science **251**, 1468 (1991).
[5] C. Lienau, A. Richter, A. Klehr, and T. Elsaesser, Appl. Phys. Lett. **69**, 2471 (1996).
[6] I. Hörsch, R. Kusche, O. Marti, B. Weigl, and K. J. Ebeling, J. Appl. Phys. **79**, 3831 (1996).
[7] T. Guenther, V. Malyarchuk, J. W. Tomm, R. Müller, and C. Lienau, Appl. Phys. Lett. **78**, 1463 (2001).
[8] S. K. Buratto, J. W. P. Hsu, E. Betzig, J. K. Trautman, R. B. Bylsma, C. C. Bahr, and M. J. Cardillo, Appl. Phys. Lett. **65**, 2654 (1994).
[9] A. Richter, J. W. Tomm, C. Lienau, and J. Luft, Appl. Phys. Lett. **69**, 3981 (1996).
[10] A. Maląg and B. Mroziewicz, J. Lightwave Technol. **14**, 514 (1996).
[11] http://www.photondesign.com
[12] G. Behme, A. Richter, M. Süptitz, and C. Lienau, Rev. Sci. Instrum. **68**, 3458 (1997).
[13] A. Kozlowska, P. Wawrzyniak, A. Maląg, M. Teodorczyk, J. W. Tomm, and F. Weik, J. Appl. Phys. **99**, 53101 (2006).
[14] M. S. Ünlü, B. B. Goldberg, W. D. Herzog, D. Sun, and E. Towe, Appl. Phys. Lett. **67**, 1862 (1995).
[15] J. Buus, IEEE J. Quantum Electron. **17**, 732 (1981).